

Quadrupole contributions to $^{10,11}\text{B} + ^{16}\text{O}$ elastic scattering

L. A. Parks,* D. P. Stanley, L. H. Courtney, and K. W. Kemper

Department of Physics, Florida State University, Tallahassee, Florida 32306

(Received 31 July 1979)

Elastic scattering angular distributions have been measured for the systems $^{10}\text{B} + ^{16}\text{O}$ at $E_L = 33.7, 41.6,$ and 49.5 MeV and $^{11}\text{B} + ^{16}\text{O}$ at $E_L = 41.6$ and 49.5 MeV. The ^{10}B and ^{11}B data are oscillatory and similar for angles less than 50° c.m. For angles greater than 50° c.m., the oscillations in the ^{10}B data are damped and the data stop decreasing with increasing angle. Elastic scattering angular distributions have been calculated for $^{11,10}\text{B} + ^{16}\text{O}$ with the coupling to the ground-state quadrupole moment included explicitly. Potentials which describe the scattering are extracted with the double folding model. It is found that the quadrupole coupling is necessary to explain the difference in ^{10}B and ^{11}B scattering from ^{16}O .

NUCLEAR REACTIONS $^{16}\text{O}(^{10}\text{B}, ^{10}\text{B})^{16}\text{O}$, $E_L = 33.7, 41.6,$ and 49.5 MeV, $^{16}\text{O}(^{11}\text{B}, ^{11}\text{B})^{16}\text{O}$, $E_L = 41.6$ and 49.5 MeV. Measured $\sigma(\theta)$, deduced Woods-Saxon, and double-folding model parameters. Coupled channels calculations for the ground-state quadrupole moment contributions.

I. INTRODUCTION

In an earlier study¹ of $^{10,11}\text{B}, ^{12}\text{C}$ scattering from ^{27}Al it was suggested that the ^{10}B ground-state quadrupole moment could be responsible for the observed differences in the angular distributions at larger angles. The possibility of contributions to the elastic scattering from the ground-state quadrupole moment of heavy-ion projectiles was first pointed out by Blair.² Scattering from the ground-state quadrupole moment will give rise to a nonspherical potential, which transfers two units of angular momentum, in addition to the normal spherical potential which acts in the elastic channel. The diagonal contributions to the angular distribution of this nonspherical potential will be "bell" shaped and out of phase with the contributions of the spherical potential.² Thus the effects of the quadrupole moment on the elastic scattering are expected to be a damping of the oscillations and with perhaps some change in magnitude of the angular distribution at larger angles.

The elastic scattering of $^{10,11}\text{B} + ^{16}\text{O}$ was undertaken to further assess the importance of ground-state quadrupole moments on the elastic scattering. This system was chosen because the more highly diffractive angular distributions expected should make the quadrupole contributions more apparent in the data. The elastic scattering data were analyzed with both the standard Woods-Saxon and double-folded potentials. Coupled channels calculations are presented for the $^{10,11}\text{B}$ ground-state quadrupole moment contributions to the elastic scattering.

II. EXPERIMENTAL PROCEDURES

A detailed description of the systems used to take the boron scattering data has been given recently,³ so that only a brief summary is required here. The $^{10,11}\text{B}$ beams were extracted from an inverted sputter source⁴ and accelerated with the Florida State University Super FN tandem Van de Graaff Accelerator. The self-supporting SiO_2 targets used had thicknesses of $110 \mu\text{g}/\text{cm}^2$ and $220 \mu\text{g}/\text{cm}^2$. The data were taken with an array of Si surface barrier detectors at forward angles and ΔE - E counter telescopes for laboratory angles $> 50^\circ$. A monitor detector was used to correct for charge collection and target thickness variations. The product of target thickness times solid angle, necessary to obtain absolute cross sections, was determined by measuring the yield of elastically scattered 4.5 MeV protons from the SiO_2 targets and assuming the cross section for this scattering previously measured by Salisbury *et al.*⁵ The cross sections are accurate to $\pm 7\%$ with the principal uncertainties arising from the extraction of the cross sections from the figures in Ref. 5, target nonuniformities, and charge integration errors.

III. ANALYSIS AND RESULTS

The data for the $^{10,11}\text{B} + ^{16}\text{O}$ elastic scattering are shown in Figs. 1 and 2. As can be seen, the ^{10}B scattering data are quite different from the ^{11}B data for angles greater than 60° c.m. The angular distributions for both projectiles are oscillatory

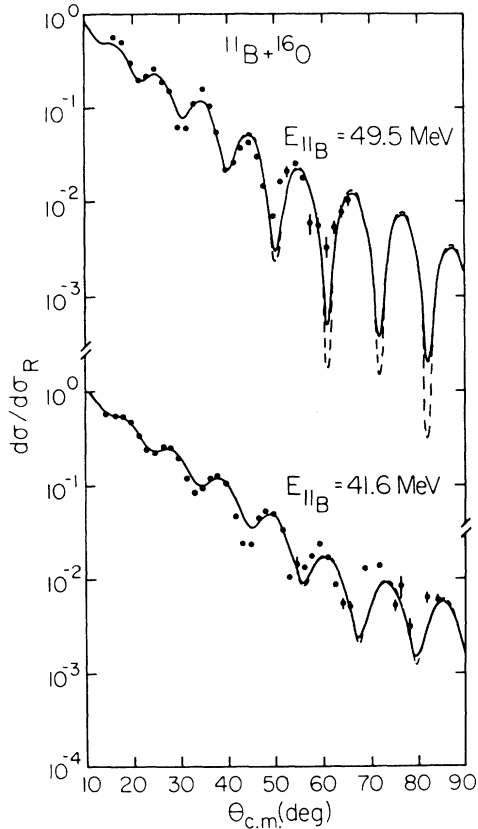


FIG. 1. $^{11}\text{B} + ^{16}\text{O}$ elastic scattering at $E_{11\text{B}} = 41.6$ and 49.5 MeV. Dashed lines are spherical optical model calculations. Solid lines are R -matrix coupled channels calculations including coupling to the ^{11}B ground-state quadrupole moment.

and decrease with increasing angle for $\sigma/\sigma_R > 5 \times 10^{-2}$, but around $\sigma/\sigma_R \approx 5 \times 10^{-2}$ the ^{10}B data stop decreasing, while the ^{11}B data continue to decrease in magnitude. This same difference in the larger angle scattering of ^{10}B and ^{11}B from $^{28,30}\text{Si}$ was observed recently.³ This difference in scattering of the ^{10}B and ^{11}B projectiles has been suggested¹ to arise because of contributions to the scattering from the large ^{10}B ground-state quadrupole moment.

Initially, attempts were made to reproduce the elastic scattering data of this work with the $1p$ shell universal optical model parameters of Towsley *et al.*⁶ The calculated angular distributions were out of phase with both the ^{10}B and ^{11}B data and did not reproduce the rate of falloff of the data. The explicit $^{10}\text{B} + ^{16}\text{O}$ parameter set of Ref. 6 gave a somewhat better description of the $^{10}\text{B} + ^{16}\text{O}$ data at smaller angles, but was still out of phase with the $^{11}\text{B} + ^{16}\text{O}$ data and failed to reproduce the $^{10}\text{B} + ^{16}\text{O}$ data at larger angles. Slight adjustments of the Ref. 6 parameters failed to yield calculated

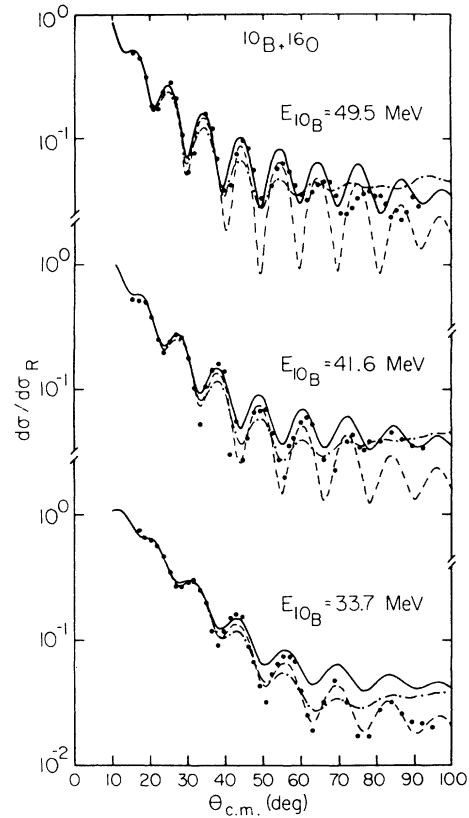


FIG. 2. $^{10}\text{B} + ^{16}\text{O}$ elastic scattering at $E_{10\text{B}} = 33.7$, 41.6 , and 49.5 MeV. Dashed lines are spherical optical model calculations. Solid lines are R -matrix coupled channels calculations including real coupling to the ^{10}B ground-state quadrupole moment. Dot-dashed lines are R -matrix coupled channels calculations including complex coupling.

angular distributions which reproduced the data.

Both double folding and Woods-Saxon form factor optical model parameter searches to reproduce the data were carried out. It was possible to get equivalent reproductions of the $^{11}\text{B} + ^{16}\text{O}$ data with both types of form factors. For the $^{10}\text{B} + ^{16}\text{O}$ data, all Woods-Saxon form factor parameter sets found which agree with the forward angle data generated oscillations greater than those seen in the larger angle data and underpredicted the data at larger angles. Real optical model potentials generated by the double folding model, which should have some physical reality, were also used to attempt to fit all of the data. However, these also failed. Although no optical potential was found in the current study which could reproduce the data, it is still possible that the data can be reproduced with a spherical optical potential which we did not find in our searches.

In order to make subsequent coupled channels calculations easier, Woods-Saxon potentials with

TABLE I. Optical model parameters. The parameter N_{DF} is the double folding renormalization factor.

$$V_{\text{W-S}}^{L=0}(\gamma) = \frac{-U}{1+e^{x_R}} - \frac{iW}{1+e^{x_I}}$$

$$V_{\text{W-S}}^{L=2}(\gamma) = -\beta \left[\frac{R_R U e^{x_R}}{(1+e^{x_R})^2} + \frac{iR_I W e^{x_I}}{(1+e^{x_I})^2} \right]$$

$$x_i = \frac{(\gamma - R_i)}{a_i} \quad (i=R, I)$$

$$R_i = r_i (A_p^{1/3} + A_t^{1/3}).$$

	N_{DF}	U (MeV)	r_R (fm)	a_R (fm)	W (MeV)	r_I (fm)	a_I (fm)	β
^{10}B	1.46	49.03	1.227	0.5232	44.37	1.305	0.302	0.260
^{11}B	1.00	28.46	1.227	0.5232	26.02	1.059	0.808	0.083

real geometry which reproduced the more physically correct double folding model potentials in the spatial region of 6 fm and beyond were found. These Woods-Saxon potentials were used to generate the angular distributions shown in Figs. 1 and 2. Since the strong absorption radius is ~ 7.5 fm, the use of Woods-Saxon potentials which reproduce double folding model potentials from 6 fm and beyond is equivalent to using the double folding model. Details of the double folding model calculations are given below. The Woods-Saxon parameters are given in Table I. In Table I, the quantity N_{DF} is the multiplicative factor by which the double folding model potentials would have to be renormalized to reproduce the data.

The $^{10}\text{B} + ^{16}\text{O}$ optical parameter set from the present study was used to calculate the cross section for 100 MeV $^{10}\text{B} + ^{16}\text{O}$. In the angular region $\theta_{\text{c.m.}} < 35^\circ$ for which data exist,⁶ the calculated cross sections provide a reasonable fit to the data; however, the angular distribution calculated with the present potentials is out of phase with the one calculated with the Ref. 6 potentials for larger angles. It would be extremely useful to measure detailed $^{11}\text{B} + ^{16}\text{O}$ scattering at 100 MeV out to the c.m. angle of 50° for the purpose of distinguishing between the different spherical potentials in Ref. 6 and the one given here, and also to determine whether an energy dependent potential is necessary.

As has been shown earlier in Ref. 1, the contribution to the elastic scattering from the ^{10}B ground-state quadrupole moment can give rise to the differences in behavior observed for ^{10}B and ^{11}B scattering by ^{16}O . Spin orbit contributions to the elastic scattering might also produce some damping of the oscillations in the $L=0$ angular distributions. However, estimates of the nucleus-nucleus spin orbit potential using the double folding model suggest that these contributions would

be small.⁷

In Ref. 1, the effect of the $L=2$ coupling potential due to the quadrupole moment was treated within the distorted-wave Born approximation (DWBA). Because the spherical ^{16}O density is smaller than the spherical ^{27}Al density, the $L=2$ potential obtained from folding with the boron quadrupole distribution is larger, relative to the $L=0$ potential, for scattering from ^{16}O than from ^{27}Al , so that the DWBA is probably insufficient for calculating the angular distributions. Consequently, the coupling between the different elastic channels is included explicitly in the present calculations. The coupled equations were solved using R -matrix techniques.⁸

The potentials used in the R -matrix coupled channels calculations were Woods-Saxon potentials which reproduce the $L=0$ and $L=2$ potentials generated by the double folding model over the spatial region ≥ 6 fm. The double folding potentials used were generated from the same boron densities and interaction as was used in Ref. 1. The equivalent Woods-Saxon potentials were used simply to reduce the number of levels necessary for convergence of the R -matrix calculations. The ^{16}O density was taken to be of an oscillator form as were the boron densities. The proton parts of the densities were taken from electron scattering.⁹ Neutron densities were assumed to be of the same shape as the proton densities. Boron ground-state

TABLE II. Charge density distribution parameters: $\rho_{\text{CH}}(\gamma) = (A + B\alpha^2\gamma^2)e^{-\alpha^2\gamma^2}$.

	A (fm ⁻³)	B (fm ⁻³)	α (fm ⁻¹)	Q (efm ²)
^{10}B	0.0796	0.0666	0.585	6.67
^{11}B	0.0839	0.0681	0.591	3.33
^{16}O	0.0704	0.1086	0.546	

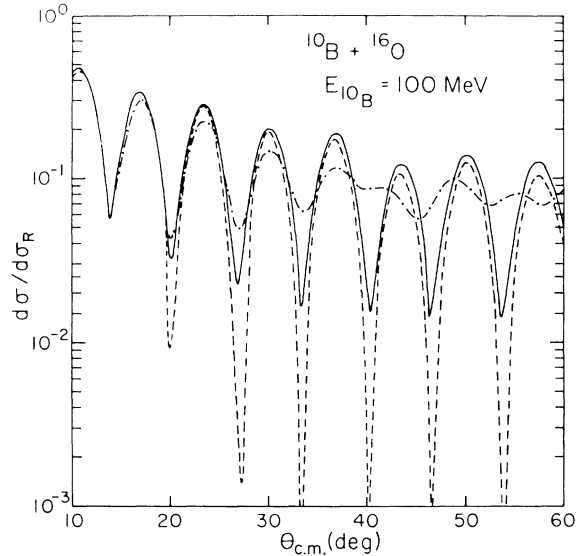


FIG. 3. Same as Fig. 2 except $E_{10B} = 100$ MeV.

quadrupole densities were taken to have a $1p$ oscillator shape and were normalized to the measured quadrupole moments. The charge density parameters used are given in Table II. The $L=2$ coupling potentials generated by the double folding model were multiplied by the same N_{DF} value as the $L=0$ double folded optical potentials. Parameters for the equivalent $L=0$ and $L=2$ Woods-Saxon potentials are listed in Table I.

Because it is not clear whether the coupling potential should be real or complex, calculations were carried out with both choices. Angular distributions for $^{10,11}\text{B} + ^{16}\text{O}$, including the $L=2$ coupling potentials are shown in Figs. 1–3. The solid line is the result with a real coupling potential and the dot-dashed line is the result with a complex coupling potential. No attempt was made to improve the quality of agreement between the calculations and experiment. Small changes in the parameters, particularly the absorption, would probably greatly improve the agreement. It is clear, however, that the addition of coupling due to the ^{10}B ground-state quadrupole moment immediately improves the agreement with experiment. Both the magnitude and amount of oscillation seen in the angular distributions at large angles are similar to those seen in the data. At 100 MeV the inclusion of the coupling potential, especially the complex coupling potential, significantly dampens the amount of oscillation at large angles, as can be seen in Fig. 3. Data currently exist⁶ only to $\theta_{c.m.} = 35^\circ$. It would be interesting to have data beyond this angle to further check the effect of the quadrupole moment on the elastic scattering. The present results are probably insufficient to determine

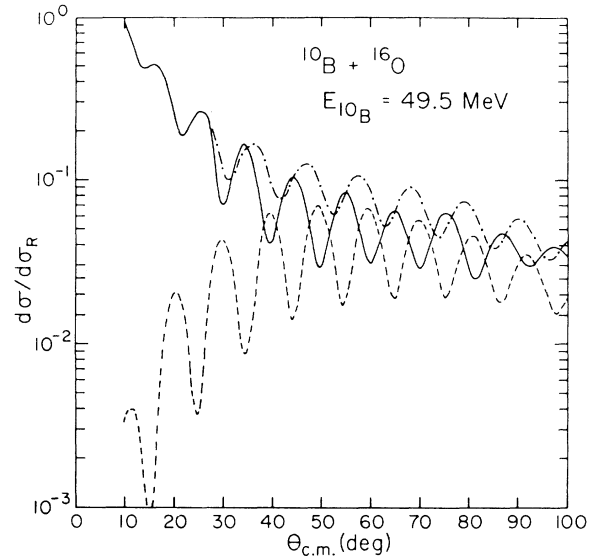


FIG. 4. Comparison of R -matrix coupled channels including real coupling (solid line) and DWBA estimate of quadrupole contribution (dot-dashed line). The dashed line is the $L=2$ contribution in the DWBA.

whether the coupling potential should be real or complex. The ^{11}B ground-state quadrupole moment has little effect on the $^{11}\text{B} + ^{16}\text{O}$ angular distribution.

If the DWBA were sufficient to estimate the effect of the quadrupole potential, the savings in computational effort over coupled channels would make use of the DWBA the obvious choice. The DWBA and R -matrix coupled channels predictions of the effect of the quadrupole potential for $^{10}\text{B} + ^{16}\text{O}$ at $E = 49.5$ MeV using a real coupling potential are shown in Fig. 4. Clearly, the DWBA is insufficient. The quadrupole potential, which is $L=2$, allows coupling between $L = J \pm 2, J$ partial waves. It is the interference between these various L values, which is neglected in the DWBA, that causes the difference between the DWBA and R -matrix coupled channels results.

IV. CONCLUSION

This work has shown that it is not possible to obtain universal optical potential parameters for the scattering between $1p$ shell nuclei as had been proposed by Towsley *et al.*⁶ Also, we have shown that results obtained for light nuclei with ^{10}B as part of the reaction system must be treated with care because of contributions from the ^{10}B ground-state quadrupole moment. It has also been shown that coupled channels calculations are necessary for determining the quadrupole contribution to the elastic scattering rather than the simpler DWBA

calculations.

The authors wish to acknowledge many useful discussions with F. Petrovich, R. J. Philpott, and D. Robson. We would like to thank R. I. Cutler

and L. H. Harwood, who assisted in data taking, and R. Leonard, who fabricated the targets. This work was supported in part by the National Science Foundation.

*Present address: IRT Corporation, San Diego, Calif. 92138.

¹L. A. Parks, K. W. Kemper, A. H. Lumpkin, R. I. Cutler, L. H. Harwood, D. Stanley, P. Nagle, and F. Petrovich, Phys. Lett. 70B, 27 (1977).

²J. S. Blair, Phys. Rev. 115, 928 (1959).

³L. A. Parks, K. W. Kemper, R. I. Cutler, and L. H. Harwood, Phys. Rev. C 19, 2206 (1979).

⁴K. R. Chapman, Nucl. Instrum. Methods 124, 299 (1975); R. I. Cutler, K. W. Kemper, and K. R. Chapman, *ibid.*

(to be published).

⁵S. R. Salisbury, G. Hardie, L. Opplinger, and R. Dangle, Phys. Rev. 126, 2143 (1962).

⁶C. W. Towsley, P. K. Bindal, K. I. Kubo, K. G. Nair, and K. Nagatani, Phys. Rev. C 15, 281 (1977).

⁷F. Petrovich, D. Stanley, L. A. Parks, and P. Nagel, Phys. Rev. C 17, 1642 (1978).

⁸R. J. Philpott, Nucl. Phys. A243, 260 (1975).

⁹C. W. de Jager, H. de Vries, and C. de Vries, At. Data Nucl. Data Tables 14, 479 (1974).